Stopped-Flow Kinetic Studies of Flavin Reduction in Human Cytochrome P450 Reductase and Its Component Domains†

Aldo Gutierrez,[||,‡] Lu-Yun Lian,[‡,¶] C. Roland Wolf,[#] Nigel S. Scrutton,*[,§] and Gordon C. K. Roberts*[,‡,||]

Centre for Mechanisms of Human Toxicity, University of Leicester, Hodgkin Building, P.O. Box 138, Lancaster Road, Leicester LE1 9HN, U.K., Biological NMR Centre, University of Leicester, Medical Sciences Building, P.O. Box 138, University Road, Leicester LE1 9HN, U.K., Department of Biochemistry, University of Leicester, University Road, Leicester LE1 7RH, U.K., and Biomedical Research Centre, University of Dundee, Ninewells Hospital and Medical School, Dundee DD1 9SY, U.K.

Received July 25, 2000; Revised Manuscript Received October 2, 2000

ABSTRACT: The reduction by NADPH of the FAD and FMN redox centers in human cytochrome P450 reductase and its component domains has been studied by rapid-mixing, stopped-flow spectroscopy. Reduction of the isolated FAD-domain occurs in three kinetically resolvable steps. The first represents the rapid formation (>500 s^{-1}) of a charge-transfer species between oxidized FAD and NADPH. This is followed by an isomerization (~ 200 s^{-1}) to a second charge-transfer species, characterized by a more intense absorption in the long-wavelength region. The third step represents hydride transfer from NADPH to FAD and is accompanied by a change in the tryptophan fluorescence of the FAD-domain. Flavin reduction is reversible, and the observed rate of hydride transfer displays a complex dependence on NADPH concentration. Two-electron-reduced FAD-domain is active in electron transfer reactions with the isolated FMN domain through the formation of a weakly associating electron transfer complex. Reduction of the CPR by NADPH occurs without direct spectral evidence for the formation of charge-transfer species, although the presence of such species is inferred indirectly. Transfer of the first hydride ion leads to the accumulation of a blue di-semiquinoid species of the reductase, indicating rapid transfer of one electron to the FMN domain. The di-semiquinoid species decays on transfer of the second hydride ion. A third phase is seen following prolonged incubation with NADPH and is assigned to a series of equilibration reactions between different redox species of the enzyme as the system relaxes to its thermodynamically most stable state. As with the isolated FAD-domain, the first hydride transfer in the reductase shows a complex dependence on NADPH concentration. At high NADPH concentration, the observed rate of hydride transfer is slow (~ 20 s^{-1}), and this attenuated rate is attributed to the reversible formation of an less active complex resulting from the binding of a second molecule of NADPH. The kinetic data are discussed with reference to the potentiometric studies on the enzyme and its component domains presented in the preceding paper in this issue [Munro, A., Noble, M., Robledo, L., Daff, S., and Chapman, S. (2001) *Biochemistry 40,* 1956−1963].

The cytochrome P450 enzymes are components of an electron-transfer chain found in the endoplasmic reticulum of eukaryotic cells which is involved in the metabolism of endogenous compounds including fatty acids, steroids, and prostaglandins and which plays a crucial role in the metabolism of drugs and xenobiotics (*2*). Cytochromes P450 are monooxygenases, and reducing equivalents required for the oxygenation reaction are provided by NADPH-cytochrome P450 reductase [CPR[1]; EC 1.6.2.4; (*3*−*7*)]. CPR is a 78-kDa membrane-bound flavoprotein, containing one molecule each of FMN and FAD (*8*), which transfers electrons from NADPH via FAD and FMN to the cytochromes P450 (*9*). The enzyme can also transfer electrons to cytochrome b_5 (*10*), haem oxygenase (*11*), and the fatty acid elongation system (*12*) and to exogenous electron acceptors including cytochrome *c* and ferricyanide (*13*, *14*). CPR can also transfer electrons to a number of drugs, including mitomycin c (*15*, *16*), adriamycin (*17*), and the benzotriazine SR4233 (*18*, *19*) and is believed to play a role in the redox cycling process by which some compounds generate reactive oxygen species in the cell.

CPR is one of only four mammalian proteins known to contain both FMN and FAD; the other examples are the isoforms of nitric oxide synthase (*20*), methionine synthase

† This work was funded by grants from the MRC and the Lister Institute of Preventive Medicine. N.S.S. is a Lister Institute Research Professor.

* To whom correspondence should be addressed: Professor G. C. K. Roberts, Telephone: +44 116 252 5533; fax: +44 116 252 5616; e-mail: gcr@le.ac.uk. Professor N. S. Scrutton, Telephone: +44 116 223 1337; fax: +44 116 252 3369; e-mail: nss4@le.ac.uk.

|| Centre for Mechanisms of Human Toxicity, University of Leicester.

‡ Biological NMR Centre, University of Leicester.

§ Department of Biochemistry, University of Leicester.

University of Dundee.

¶ Current address: Department of Biomolecular Sciences, University of Manchester Institute of Science and Technology, Manchester M60 1QD UK.

[1] Abbreviations: CPR, cytochrome P450 reductase; NOS, nitric oxide synthase; FRET, fluorescence resonance energy transfer.

10.1021/bi001719m CCC: $20.00
Published on Web 01/03/2001

reductase (*21*), and protein NR1 (*22*). Sequence analysis and a range of biochemical studies show that it comprises three separable domains: a hydrophobic N-terminal domain that anchors the enzyme to the endoplasmic reticulum membrane, an FMN-binding domain, and an FAD/NADPH-binding domain (*5*, *23*−*26*). This has been confirmed by the determination of the structure of rat liver CPR (lacking the N-terminal membrane anchor) at 2.6 Å resolution by X-ray crystallography (*27*); the 1.93 Å X-ray crystal (*28*) and NMR solution (*29*) structures of the isolated FMN-binding domain of human CPR have also been determined. The FMN-binding domain is structurally strikingly similar to flavodoxins (*30*) and is linked to the FAD-domain by a flexible loop. The C-terminal part of the protein consists of a FAD- and NADPH-binding domain, structurally related to the equivalent domains found in ferredoxin-$NADP^+$ reductase (FNR) (*31*), with, as an insert, an additional domain that may serve to orient the FAD- and FMN-binding domains optimally for intramolecular electron transfer. In the crystal structure of rat CPR, the isoalloxazine rings of the two flavin centers are separated by a distance of only 4 Å and the expectation, therefore, is that intramolecular electron transfer between the FAD and FMN centers is rapid.

CPR from nonhuman sources has been the subject of a number of potentiometric (*32*) and kinetic studies (*33*−*35*) that have established the redox potentials of the flavin cofactors and the principle redox states of the enzyme during catalysis. Flash photolysis has also been used in an attempt to probe the kinetics of intramolecular electron transfer between the flavin redox centers (*36*). Although CPR is of central importance in the metabolism of drugs and xenobiotics in man, studies of electron transfer in the human enzyme have been lacking. We now report a detailed kinetic study of electron flow through human CPR. The individual FAD- and FMN-binding domains of human CPR have been separately expressed (*24*), and we have therefore extended our kinetic analyses to include studies of electron transfer in these isolated domains. This reductionist approach has facilitated the deconvolution of spectral and kinetic properties of the CPR enzyme, in addition to providing new information concerning the mechanism of hydride transfer in the FAD-domain. Together with the potentiometric studies reported in the preceding paper in this issue (*1*), our work provides the first detailed mechanistic account of electron transfer in this complex human flavoprotein.

EXPERIMENTAL PROCEDURES

Protein Purification. Human fibroblast CPR (lacking the N-terminal membrane-anchoring domain) and its two functional domains, the NADPH/FAD-binding domain (exons 8−16) and FMN-binding domain (exons 3−8), were expressed in *Escherichia coli* BL21(DE3)pLysS from appropriate pET15b plasmid constructs and purified as described earlier (*24*, *29*, *37*, *38*). The NADPH/FAD-binding domain (hereafter referred to as FAD-domain) was purified using the protocol described for full-length CPR (*38*). Nickel-agarose affinity and ion-exchange chromatography were used to purify the FMN domain as described previously (*29*), but EDTA was omitted during the ion-exchange step to avoid photoreduction of the protein. The His-tag was removed by thrombin cleavage. Purified proteins were treated with potassium hexacyanoferrate (III) and incubated overnight with a 5−10 molar excess of free FAD and/or FMN. Following exhaustive dialysis, the proteins were concentrated and stored at −20 °C in 50 mM potassium phosphate buffer, pH 7.0, containing 50% glycerol; they were stable under these conditions for periods of up to 1 year. The cofactor content of the enzymes was determined by reverse-phase HPLC (*39*) using a Waters ODS2 column (4.6 × 250 nm), which showed that the purification procedures used yielded enzymes assembled stoichiometrically with their constituent cofactors. Protein concentration was determined using the following molar extinction coefficients (M^{-1} cm^{-1}) at 450 nm, determined using the method described (*40*): CPR 22 000; FMN-domain 12 200; FAD-domain 11 300.

For studies of hydride transfer from the two-electron-reduced FAD-domain to $NADP^+$, the FAD-domain was prereduced stoichoimetrically with dithionite in the presence of methyl viologen as a redox mediator. The molar ratio of FAD-domain to methyl viologen was 10. Anaerobic dithionite solution was titrated against free FAD in 50 mM potassium phosphate buffer, pH 7.0, using methyl viologen as an indicator. For studies of interdomain electron transfer, the FAD-domain was reduced to the two-electron level by the addition of a 20-fold molar excess of NADPH under anaerobic conditions. The sample was allowed to reach equilibrium (∼10 min incubation), and the cofactor was then removed by rapid gel filtration. Reduced FAD-domain was then used immediately in stopped-flow studies.

Kinetic Measurements. Single turnover studies were performed using an Applied Photophysics SX.17 MV stopped-flow spectrophotometer. Unless otherwise stated, measurements were carried out at 25 °C in 50 mM potassium phosphate buffer, pH 7.0. Protein concentration was 10 μM (reaction cell concentration) unless stated otherwise, and reactions were performed under anaerobic conditions. The sample-handling unit of the stopped-flow instrument was contained within a Belle Technology glovebox, as described (*41*). All buffers were made oxygen-free by evacuation and extensive bubbling with argon before use. Prior to stopped-flow studies, protein samples were treated with potassium hexacyanoferrate, and excess cyanoferrate was removed by rapid gel filtration (Sephadex G25).

Stopped-flow, multiple-wavelength absorption studies were carried out using a photodiode array detector and X-SCAN software (Applied Photophysics Ltd). Spectral deconvolution was performed by global analysis and numerical integration methods using PROKIN software (Applied Photophysics Ltd). In single wavelength studies, flavin reduction by NADPH was observed at 450 nm; transients were found to be biphasic with both CPR and the FAD-domain and were fitted using the standard double exponential expression (eq 1). where k_{obs1} and k_{obs2} are the observed rate constants for

$$A_{450} = C_1 e^{-k_{obs1}t} + C_2 e^{-k_{obs2}t} + b \qquad (1)$$

the faster and slower phases, respectively, C_1 and C_2 are their relative amplitudes values, and b is the final absorbance. Electron transfer from FAD to FMN within two-electron-reduced CPR gives rise to the appearance of a blue di-semiquinoid enzyme species with an optical signature centered at 600 nm. A second hydride transfer from NADPH produces the fully reduced hydroquinone species, which is associated with a bleaching of absorbance at 600 nm.

Transients at 600 nm reporting on this formation and decay of the blue di-semiquinoid species were analyzed using eq 2:

$$A_{600} = \frac{k_{obs1}}{k_{obs2} - k_{obs1}} C(e^{-k_{obs1}t} - e^{-k_{obs2}t}) + b \qquad (2)$$

where k_{obs1} and k_{obs2} are observed rate constants for the formation and decay of the blue di-semiquinoid intermediate, respectively, C is the amplitude term, and b is an off-set value.

Stopped-flow fluorescence experiments employed excitation wavelengths of 295 nm (protein tryptophans) or 340 nm (NADPH); emission bands were selected using band-pass filters (Coherent Optics; 350 nm #35-3003, 450 nm #35-3367).

Steady-state measurements were performed in a Hewlett-Packard 8452A single-beam diode array spectrophotometer using a 1-cm light path. The desired concentrations of NADPH and horse cytochrome *c* were obtained by making microliter additions from stock solutions to the assay mix. Reactions were performed at 25 °C in 50 mM potassium phosphate buffer, pH 7.0.

RESULTS

Stopped-Flow Studies of the Isolated FAD-Domain. The reductive half-reaction of the isolated FAD-domain was studied by stopped-flow spectroscopy at 25 °C, following enzyme reduction after rapid mixing with NADPH by photodiode array detection (Figure 1, panel A). The spectra as a function of time were fitted globally by numerical integration methods using Prokin software (Applied Photophysics). Data collected over a period of 2 s from the mixing event were best fitted to a one-step model (A → B; Figure 1) with a rate of conversion of 2.5 s^{-1}. Species A (spectrum a in Figure 1, panel B) has an increased and broad absorption peak at 550−700 nm, indicative of NADPH−FAD charge-transfer species. The high absorption at ∼450 nm in spectrum a indicates that the flavin is in the oxidized form. The oxidized and nonliganded FAD-domain does not absorb in the long-wavelength region (550−700 nm), and the data thus suggest that formation of this charge-transfer species (species A) occurs predominantly within the first 3.8 ms of the reaction (i.e., before the first spectrum is recorded). Consistent with this, a plot of the concentration of spectrally defined enzyme species versus time derived from the global fitting process indicates that the charge-transfer species is essentially the only enzyme species present at the time when the first spectrum is recorded (Figure 1, panel B inset). In spectrum b in Figure 1, panel B, corresponding to the species that predominates at >1 s, the charge-transfer absorption at 550−700 nm is lost, and the absorption at 450 nm is substantially bleached, indicating flavin reduction. The residual absorbance at 450 nm in spectrum b indicates that flavin reduction by NADPH is not complete, suggesting that hydride anion transfer to the flavin is reversible (see also below).

The diode array data indicate that the formation of a charge-transfer complex occurs quickly, i.e., within the first 3.8 ms after the mixing event. The earliest point of data collection using the photodiode array is restricted by the

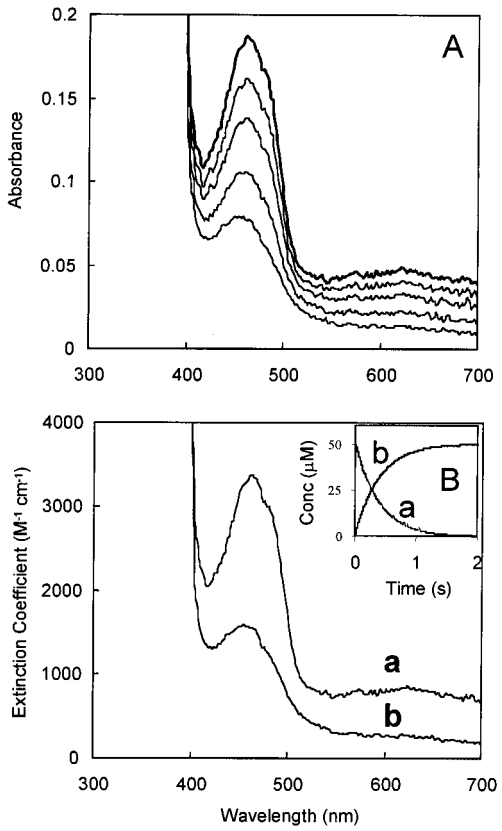

FIGURE 1: Reaction of the isolated FAD-domain of human cytochrome P450 reductase with NADPH monitored by stopped-flow photodiode array spectroscopy. Conditions: 50 mM potassium phosphate buffer, pH 7.0, 25 °C. [FAD-domain] 50 μM, [NADPH] 1 mM. Panel A, time-dependent spectral changes on rapidly mixing the FAD-domain with NADPH. The experiment was performed over 2 s after the initial mixing event. The first spectrum is recorded 3.8 ms after mixing; for clarity, only selected subsequent spectra are shown. Panel B, denconvoluted spectra for the reaction shown in panel A. The data shown in panel A were fitted to the model A → B. The observed rate for the conversion of A → B (obtained from global fitting) is 2.54 s^{-1}. Inset: calculated concentration profiles (over 2 s) of intermediates in the reaction of isolated FAD-domain with NADPH. Profiles were obtained by fitting the data shown in panel A to a sequential A → B kinetic scheme.

photodiode itself and not the dead-time of the stopped-flow instrument (1.2 ms), and it is thus possible to obtain data from 1.2 ms in single wavelength mode using a conventional photomultiplier. Also, a decrease in the enzyme concentration from 50 μM (used in the photodiode array experiments) to 10 μM for the single wavelength studies would be expected to decrease the rate of formation of the charge-transfer intermediate. Single-wavelength stopped-flow studies at 450 nm revealed a biphasic kinetic transient (Figure 2, panel A), and the observed rate for the slow kinetic phase (3.5 s^{-1}) is in reasonable agreement with that calculated globally from the photodiode array data (Figure 1, panel B). The rate observed for the fast phase at 450 nm is 202 s^{-1}. Single-wavelength analysis at 600 nm (over a period of 2 s from the mixing event) revealed an initial rapid increase in absorbance, followed by a slower decrease, reflecting the formation and subsequent decay of a charge-transfer species (Figure 2, panel B). However, recording the reaction over shorter time periods (20 ms) indicated that the initial increase in absorbance is biphasic, revealing the existence of two discrete charge-transfer species, CT1 and CT2 (Figure 2,

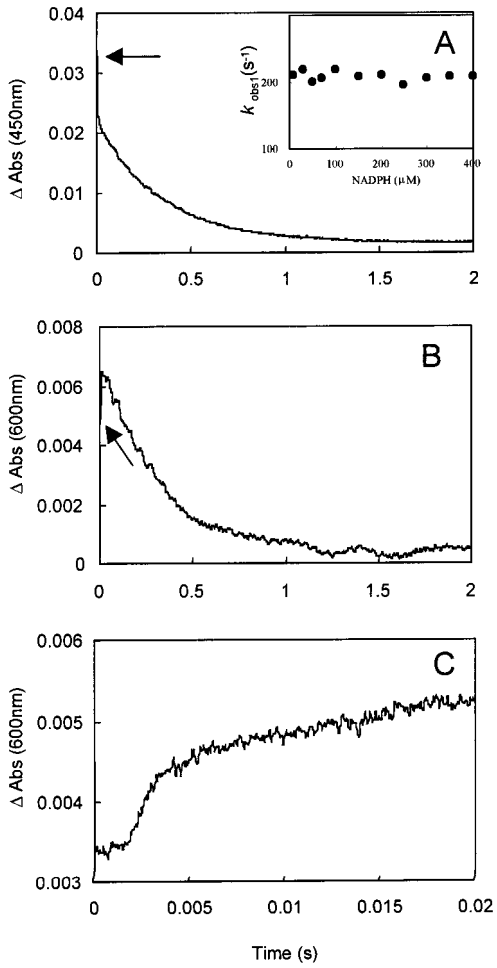

FIGURE 2: Transients obtained for the FAD-domain in single wavelength studies of flavin reduction by NADPH. Conditions: 50 mM potassium phosphate buffer, pH 7.0, 25 °C. [FAD-domain] 10 μM, [NADPH] 200 μM. Panel A, biphasic transient observed at 450 nm. Fitting to eq 1 yields values for k_{obs1} and k_{obs2} of 202 and 3.5 s^{-1}, respectively. Inset: [NADPH] dependence of k_{obs1}. Panel B, transient obtained at 600 nm. Fitting the "down" phase to a monophasic expression yields a value for the observed rate constant of 3.2 s^{-1}. Panel C, as for panel B, but reaction monitored over 20 ms to illustrate the presence of two kinetic phases inferred to represent the accumulation of two discrete charge-transfer species. Arrows indicate the initial absorbance values for the kinetic transients.

panel C). Note that in Figure 2, panels B and C, the initial measured absorbance is higher than the final absorbance on completion of the "decay" phase. This indicates that the formation of the first charge-transfer species (CT1) is fast (>500 s^{-1}) and is almost complete within the dead-time of the stopped-flow instrument. This species is presumably the initial result of NADPH binding to oxidized FAD-domain. The observed rate of formation of CT1 should therefore be dependent on the NADPH concentration, but the fast rate of formation of this species prevented detailed analysis of its concentration dependence. The observed rate (500 s^{-1}) for formation of CT1 applies to an NADPH concentration of 200 μM. The rate constant for formation of CT1 is likely to be second order.

The rate of formation of the second charge-transfer species (CT2) measured at 600 nm is identical to the first phase of absorbance change observed at 450 nm, indicating that both wavelengths report on the same kinetic step. The observed rates of this step are independent of NADPH concentration (Figure 2, panel A, inset), consistent with the sequential kinetic scheme for the reductive half-reaction developed below (Scheme 1). The rates of the slow phase of the 450 nm transient and of the slowest (absorbance decrease) of the three phases in the 600 nm transient are also independent of NADPH concentration in the pseudo-first-order regime but show an unusual concentration dependence at <100 μM NADPH (see Figure 5 below). The two slow kinetic phases at 450 and 600 nm clearly report on the same kinetic step, and the spectral changes are consistent with hydride anion transfer from NADPH to the FAD.

The hydride transfer step was also followed by stopped-flow fluorescence analysis, making use of the decrease in NADPH fluorescence (excitation 340 nm, emission 450 nm) on hydride transfer. Rapid mixing of NADPH with the FAD-domain resulted in a decrease in fluorescence emission (Figure 3, panel A), the observed rate being similar to that seen for flavin reduction in the stopped-flow absorption studies described above (Figure 2, panel A).

The crystal structure of rat CPR indicates that a tryptophan residue (Trp-677) is positioned close to the isoalloxazine ring of the flavin in the FAD-domain (*27*). This residue is conserved in human cytochrome P450 reductase as Trp-676. In the structure of the oxidized rat enzyme, the *re*-face of the flavin is protected by Trp-677, which prevents close interaction of the nicotinamide cofactor with the flavin isoalloxazine. To enable nicotinamide binding and subsequent hydride transfer, the side chain of Trp-677 (and by inference Trp-676 in the human enzyme) must swing away from the flavin. The proximity of Trp-676 to the flavin and nicotinamide cofactor and the conjectured movement of the tryptophan side chain suggested that a change in the fluorescence characteristics of this tryptophan side chain might be observed on NADPH binding and hydride transfer. Both tryptophan fluorescence (excitation 295 nm, emission 340 nm; Figure 3, panel B) and fluorescence resonance energy transfer (FRET) from the tryptophan to the reduced nicotinamide (excitation 295 nm, emission 450 nm; Figure 3, panel C) were examined, and both were found to show a biphasic behavior. An initial rapid increase in tryptophan fluorescence and in FRET occurs at a rate similar to those associated with the formation of the CT2 species in stopped-flow absorption studies (see above), showing that the formation of this species is associated with a change in the environment of one or more tryptophan residues, most probably Trp-676. The tryptophan fluorescence and the FRET then decrease with an observed rate identical to the change in nicotinamide fluorescence and flavin absorbance identified with hydride transfer (Figure 3, panels B and C).

Reversibility of Hydride Transfer with the FAD-Domain. In the preceding paper in this issue (*1*), Munro and co-workers report that the $FADH^{\bullet}/FADH_2$ couple has a very low midpoint potential (−371 mV); however, the effect of NADPH binding on the flavin reduction potential is not known. The potential of the $FAD/FADH_2$ couple of spinach ferredoxin-$NADP^+$ reductase, which is structurally related to the FAD-domain of CPR (*23*, *27*, *31*) is raised from −376 to −300 mV on the binding of $NADP^+$ to form an enzyme−$NADP^+$ charge-transfer complex (*42*). Thus, the binding of NADPH to the FAD-domain of human P450 reductase may elicit a perturbation in the reduction potential of the flavin.

Scheme 1

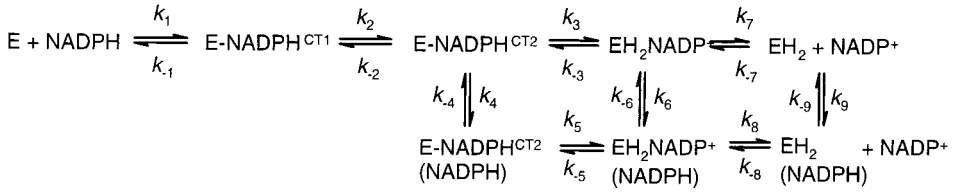

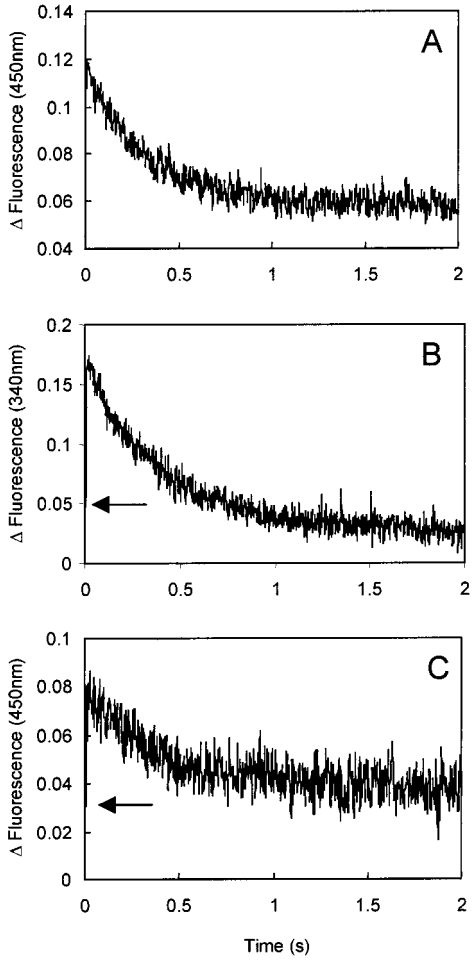

FIGURE 3: Fluorescence kinetic transients obtained for the reduction of the FAD-domain by NADPH. Conditions as for Figure 2. (A) Decrease in fluorescence emission at 450 nm following excitation at 340 nm, illustrating the kinetics of hydride anion transfer; (B) decrease in tryptophan fluorescence emission at 340 nm following excitation at 295 nm; (C) decrease in FRET between tryptophan and NADPH as a result of hydride anion transfer to the FAD. Arrows indicate the presence of a very rapid increase in fluorescence emission in transients B and C. This rapid increase in fluorescence is not seen in transient A (see text for details).

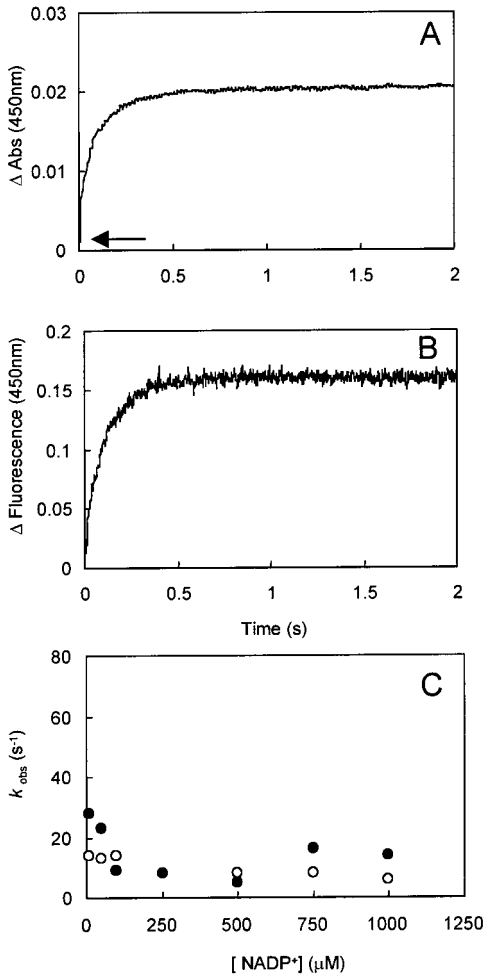

FIGURE 4: Absorption and fluorescence transients for the reaction of two-electron reduced FAD-domain with $NADP^+$ and dependence of hydride transfer rate on [$NADP^+$]. Conditions: potassium phosphate buffer, pH 7.0, 25 °C. [reduced FAD-domain] 10 μM. (A) Absorption transient observed at 450 nm; [$NADP^+$] 250 μM; (B) fluorescence transient observed at 450 nm with excitation at 340 nm; [$NADP^+$] 250 μM; (C) dependence of observed rate of hydride transfer on [$NADP^+$]. Open circles, fluorescence data; filled circles, absorption data. The arrow in panel A illustrates the beginning of the rapid phase of the absorption transient.

Our stopped-flow absorption studies using photodiode array detection indicate that flavin reduction was not complete on mixing the FAD-domain with a 20-fold excess of NADPH (Figure 1, panel A). A similar observation has been made under equilibrium conditions (data not shown). Our data are consistent with the known values of the midpoint reduction potentials of the flavin and nicotinamide coenzyme couples. Any increase in the potential of the FAD cofactor in the FAD-domain on binding NADPH (as seen with FNR) would serve to displace the position of the equilibrium further toward oxidized FAD-domain.

To investigate the reversibility of hydride transfer, stopped-flow studies were performed in which two-electron-reduced FAD-domain (generated by titration with dithionite) was rapidly mixed with $NADP^+$. Kinetic transients observed at 450 nm are biphasic (Figure 4, panel A). The fast phase most likely represents a reduced FAD-$NADP^+$ charge-transfer species (as seen in spinach ferredoxin-$NADP^+$ reductase; *42*), whereas the slow phase ($\sim$8 s^{-1}) represents hydride transfer from the flavin to $NADP^+$. Further evidence for this latter assignment was obtained from fluorescence stopped-flow studies, in which an increase in fluorescence emission at 450 nm (indicating hydride transfer to $NADP^+$) was seen with the same observed rate as that of the slow phase of the absorption change at 450 nm (Figure 4, panel B). The

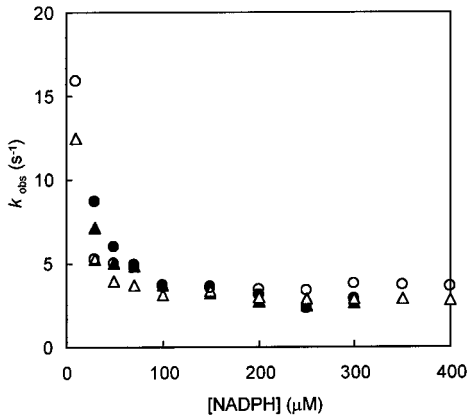

FIGURE 5: Dependence of the observed rates of hydride anion transfer and CT2 decay in FAD-domain on [NADPH] measured by absorption and fluorescence stopped-flow. (○) Absorption at 600 nm; (△) absorption at 450 nm; (●) FRET monitored at 450 nm; (▲) hydride anion transfer monitored as a fluorescence decrease at 450 nm.

observed rate of hydride transfer measured in stopped-flow absorption and fluorescence mode was found to be essentially independent of [$NADP^+$] in the pseudo-first-order regime (Figure 4, panel C).

Kinetic Scheme for Reduction of the FAD-Domain. On the basis of the kinetic data presented above for the isolated FAD-domain, it is possible to construct a kinetic scheme for reduction of the FAD by NADPH (Scheme 1). Scheme 1 indicates the presence of intermediates for which evidence has been acquired in the kinetic studies described in this paper. The forward reaction involves the sequential formation of two discrete charge-transfer species (CT1 and CT2). Formation of the charge-transfer intermediates is likely to be reversible. The hydride transfer step is slow (under pseudo-first-order conditions, observed rate $\sim 3\ s^{-1}$), and since this is a reversible reaction, the observed rate describes the approach to equilibrium, and its value is dependent on the microscopic rate constants describing the equilibrium distribution. An unusual aspect of the reductive half-reaction is the finding that the observed rate of hydride ion transfer from NADPH to FAD (as followed by absorption and fluorescence spectroscopy) *increases* as the NADPH concentration is decreased below 100 μM (Figure 5). This contrasts with the data in the pseudo-first-order regime (with NADPH in >10-fold excess over protein), where the rates are independent of NADPH concentration (Figure 5). The enhanced rates of hydride transfer at low NADPH concentration are inconsistent with a reversible, linear scheme involving the binding of NADPH to the FAD-domain followed by hydride transfer to the flavin, which would predict a decrease in observed rate as the NADPH concentration is lowered (since the rate would be limited by the second-order binding of coenzyme to the FAD-domain). The minimal kinetic scheme required to explain the data involves the binding of a second molecule of NADPH to form a complex in which the rate of hydride transfer is decreased (Scheme 1). This species is shown as being formed from the CT2 species since the rate of formation of CT2 is independent of NADPH concentration even in the low concentration regime. The mode of binding of this second NADPH molecule is as yet unknown. It is interesting that in the crystal structure of rat CPR (*27*) the electron density of the ribose-nicotinamide portion of the bound $NADP^+$ is low, and indicative of different modes of binding in the two molecules of the asymmetric unit, neither of which are appropriate for hydride transfer to FAD. This at least indicates that nonproductive modes of binding of the nicotinamide ring to CPR can exist.

Electron Transfer from the Isolated FAD-Domain to the FMN Domain. Having demonstrated that the isolated FAD-domain is functionally active in its ability to accept reducing equivalents from NADPH, it was of interest to ascertain if the reduced FAD-domain can pass electrons to the isolated FMN-domain of human CPR. Titrations of (i) CPR lacking the membrane anchor region and (ii) the component domains with NADPH are shown in Figure 6, panels A and B.[2] The titrations reveal that the spectral changes accompanying reduction of CPR or its component domains are very similar. The data indicate that the level of reduction is similar in each case, from which one can infer that the thermodynamic equilibrium (in terms of distribution of reducing equivalents) following the reductive titration is similar. No spectral changes were observed on the mixing of the isolated oxidized FAD-domain with the isolated oxidized FMN-domain (Figure 6, panel C). This observation indicates either (i) a lack of any structural perturbation that influences the flavin environment on formation of the complex of the two domains or (ii) an association constant for complex formation that is too small to generate sufficient complex under equilibrium conditions. NMR studies of the effects of adding the FAD-domain to ^{15}N-labeled FMN-domain revealed no chemical shift changes indicative of complex formation, consistent with a weak association (B. Hawkins, L.-Y. Lian, G. C. K. Roberts, unpublished results). The kinetics of interdomain electron transfer were studied by mixing the FAD-domain (prereduced to the level of two electrons with NADPH) with the isolated FMN-domain and following the changes in absorbance at 450 nm and 600 nm. A linear dependence of the observed rate of electron transfer on the concentration of the FMN-domain was observed (Figure 6, panel D), again implying that a stable complex between the two domains is not formed and that the observed electron transfer rates are primarily controlled by the rate of complex assembly; the data in Figure 6, panel D, yield an estimate of $9.5 \times 10^4\ M^{-1}\ s^{-1}$ for the second-order rate constant. Comparable data were also obtained at 600 nm, where electron transfer gives rise to a monophasic increase in absorbance due to the formation of the blue di-semiquionoid species of the constituent domains (data not shown).

Stopped-Flow Studies of CPR. Stopped-flow experiments with absorbance and fluorescence detection were used to investigate the mechanism of electron transfer in human CPR, intact except that it lacked the N-terminal membrane anchor. As with the FAD-domain, photodiode array analysis of the absorbance changes following mixing of the enzyme with NADPH indicated incomplete reduction of the flavins (i.e.,

[2] The final spectra obtained under equilibrium conditions differ from those observed following flavin reduction by NADPH in stopped-flow experiments using the photodiode array (2 s after mixing; Figure 7). This arises because prolonged incubation of CPR (and its component domains) with NADPH gives rise to spectral changes over a period of about 100 s associated with equilibration of the reduced enzyme species. These spectral changes are manifest as an increase in absorption at 600 nm and a further decrease in absorption at 450 nm (see section on CPR kinetics for further discussion).

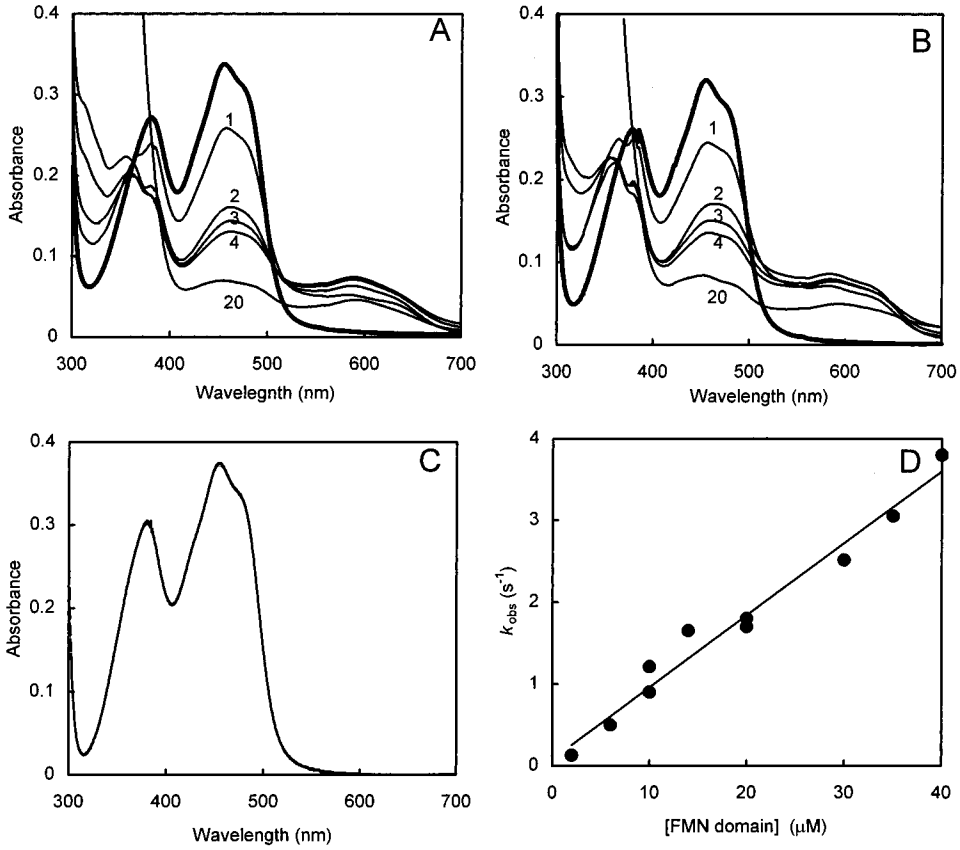

FIGURE 6: Spectra of CPR and mixtures of the FMN- and FAD-domains in the oxidized and reduced form and rates of electron transfer between the constituent domains. Conditions: 50 mM potassium phosphate buffer, pH 7.0, 25 °C. Panel A, spectral changes accompanying the titration of CPR (15 μM) with NADPH. Numbers indicate hydride equivalents added in the form of NADPH. Panel B, spectral changes accompanying the titration of a mixture of FAD-domain (15 μM) and FMN-domain (15 μM) with NADPH. Numbers indicate hydride equivalents added in the form of NADPH. Panel C, spectrum of FAD-domain (15 μM) and FMN domain (15 μM) before and after mixing in a Yankeelov optical cell. The two spectra are essentially superimposable. Panel D, observed rate of electron transfer (measured at 450 nm as a monophasic decrease in absorbance) between two-electron-reduced FAD-domain and oxidized FMN-domain. The data are shown fitted to a linear dependence described by a second-order rate constant of 9.5×10^4 M^{-1} s^{-1}. The concentration of the FAD-domain was 2 μM.

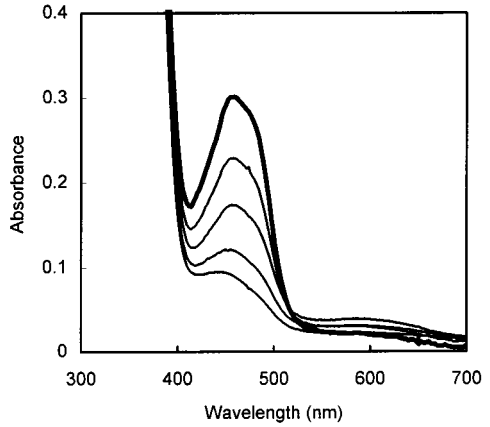

FIGURE 7: Reaction of human CPR (lacking the membrane anchor) with NADPH monitored by stopped-flow photodiode array spectroscopy. Conditions: 50 mM potassium phosphate buffer, pH 7.0, 25 °C. [CPR] 20 μM, [NADPH] 400 μM. The experiment was performed over 2 s after the initial mixing event. The first spectrum is recorded 3.8 ms after mixing; for clarity, only selected subsequent spectra are shown.

incomplete bleaching of the 450 nm absorption) (Figure 7). With full-length CPR, no evidence was observed for a fast charge-transfer step, comparable to that seen with the FAD-domain, in photodiode array single-wavelength studies (at 450 or 600 nm; Figure 8, panels A and B). However, in CPR a slower ($\sim$20 s^{-1}) and larger increase in absorption was seen at 600 nm, which coincided with the faster of the two phases observed at 450 nm (flavin reduction; see below) (Figure 8, panel B). Rather than representing a transient charge-transfer species, we attribute this increase in absorbance at 600 nm to the formation of neutral ("blue") flavin semiquinone. The inference is, therefore, that following hydride transfer to the FAD, there is a rapid transfer of one electron to the FMN, giving rise to the blue semiquinone signal corresponding to CPR in the blue di-semiquinonoid (FADH•/FMNH•) state. This is consistent with the large driving force for electron-transfer calculated from the midpoint potentials of the $FAD_{sq/red}$ couple (−382 mV) and the $FMN_{ox/sq}$ couple (−66 mV) (*1*). The transfer of a second electron to FMNH• in two-electron-reduced reductase is much less favorable, since the $FAD_{ox/sq}$ and $FMN_{sq/red}$ couples are essentially isopotential (−283 and −269 mV, respectively; *1*).

The slow, decreasing absorbance phase of the 600 nm transient (Figure 8, panel B) represents conversion of the two-electron-reduced reductase to a four-electron-reduced species, with loss of the blue flavin semiquinone signature. The rate of this phase is equivalent to the rate of the slow (second) phase of the 450 nm transient, representing further reduction of the flavin (Figure 8, panel A). Confirmation

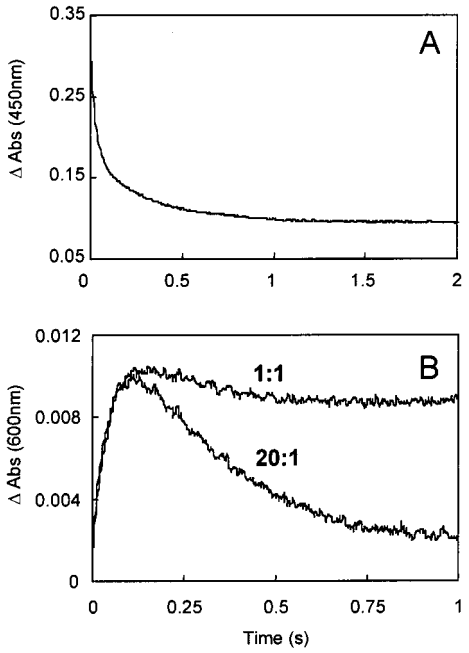

FIGURE 8: Transients obtained for CPR in single wavelength studies of flavin reduction by NADPH. Conditions: 50 mM potassium phosphate buffer, pH 7.0, 25 °C. [CPR] 10 μM, [NADPH] 200 μM. Panel A, transient observed at 450 nm. Data are best described by a double exponential expression (eq 1), yielding values for k_{obs1} and k_{obs2} of 20 and 3.7 s^{-1}, respectively. Panel B, transients observed at 600 nm. Ratios indicate relative concentrations of CPR and NADPH. For the transient shown with a 20:1 ratio of NADPH/CPR, the data were fitted using eq 2, yielding values for k_{obs1} and k_{obs2} of 20 and 3.5 s^{-1}, respectively.

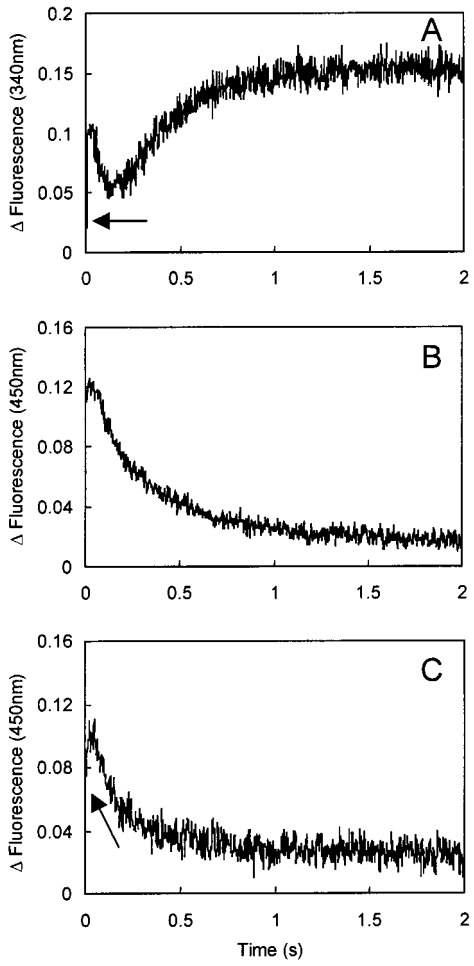

FIGURE 9: Fluorescence kinetic transients obtained for the reduction of CPR by NADPH. Conditions as for Figure 8. (A) Changes in tryptophan fluorescence emission at 340 nm following excitation at 295 nm; (B) decrease in fluorescence emission at 450 nm following excitation at 340 nm, illustrating the kinetics of hydride anion transfer; (C) decrease in FRET between tryptophan and NADPH as a result of hydride anion transfer to the FAD. Arrows indicate the presence of a very rapid increase in fluorescence emission in transients A and C. This rapid increase in fluorescence is not seen in transient B (see text for details).

that the loss of signal at 600 nm is due to loss of a blue semiquinone signal was obtained by mixing CPR with a stoichiometric amount of NADPH (Figure 8, panel B). In this case, the blue semiquinone forms, but there is very little decay of its characteristic absorbance as compared with reactions performed with excess NADPH (Figure 8, panel B). These data confirm that the absorption changes seen at 600 nm are not due to the transient formation of a charge-transfer species.

The reductive half-reaction of CPR was also followed by stopped-flow fluorescence analysis, as described for the FAD-domain (see above). The transient obtained at an emission wavelength of 340 nm (excitation 295 nm, tryptophan fluorescence; Figure 9) is more complex than that seen with the isolated FAD-domain (Figure 3). With the FAD-domain, we observed a very rapid increase in fluorescence emission (which we attribute to movement of a tryptophan side-chain on binding NADPH), followed by a reduction in fluorescence with kinetics identical to hydride transfer. In CPR, however, the early part of the transient is complex (Figure 9, panel A). Initially, there is a rapid increase in fluorescence (as with the FAD-domain, and similarly attributed to an NADPH-induced conformational change) followed by a decrease in fluorescence ($\sim$20 s^{-1}) with kinetics similar to that of hydride transfer to form the two-electron-reduced form of CPR. There is then a slower increase in fluorescence emission (3 s^{-1}), the kinetics of which mirror the transfer of the second hydride anion to the enzyme. This second hydride transfer occurs at a rate similar to that seen for reduction of the isolated FAD-domain by NADPH. This observation implies that the rate of release of $NADP^+$ does not limit the rate of the second hydride transfer reaction in full-length CPR. The transients observed for NADPH oxidation (excitation 340 nm; emission 450 nm) and for FRET between tryptophan and NADPH (excitation 295 nm; emission 450 nm) are initially complex in the early time domain (0 to 20 ms) but approximate to monophasic at longer time excursions (100 ms to 2 s) (Figure 9, panels B and C, respectively). The "monophasic" portion is similar in rate to that of the transfer of the second hydride anion (determined from absorption studies) to form four-electron-reduced reductase. The complexities occurring in the initial parts of the transients (described above) prevent accurate analysis of the fluorescence decrease in the $\sim$20 to 100 ms time scale to obtain the rate of transfer of the first hydride anion. However, visual comparison of the transient shown in Figure 9, panel A, with those shown in Figure 9, panels B and C, indicates that the expected fluorescence decrease for NADPH oxidation (in the $\sim$20 to 100 ms time domain) correlates well with the observed decrease in tryptophan fluorescence. This provides additional evidence that this decrease in tryptophan fluorescence reports on the transfer

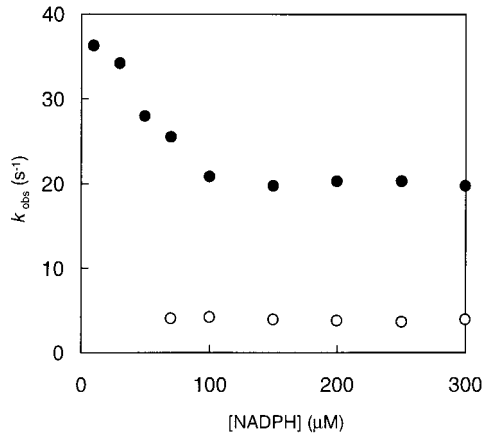

FIGURE 10: Dependence of the observed rates on [NADPH] for the first and second hydride anion transfer in CPR measured by absorption stopped-flow experiments. (●) Observed rate for the first hydride transfer inferred from the rate of formation of the blue semiquinone (observed at 600 nm). Note the enhancement in rate at [NADPH] < 100 μM; (○) observed rate for the second hydride transfer measured at 450 nm (slow phase); similar data were obtained at 600 nm (slow phase). Data for the second hydride transfer cannot be obtained below 100 μM NADPH due to loss of absorption signal (see text for details).

of the first hydride anion (Figure 9, panel A).

The [NADPH] dependencies of the various phases obtained from absorption and fluorescence studies are shown in Figure 10. As seen with the FAD-domain, hydride transfer rates were found to be independent of [NADPH] in the pseudo-first-order regime. The observed rate of the first hydride transfer in CPR is presumably faster than that of the second hydride transfer (or indeed the hydride transfer to the FAD-domain alone) because of the ability of the FMN cofactor to rapidly accept an electron and thus suppress the reverse transfer step (i.e., from $FADH_2$ to $NADP^+$). Similar reasoning explains why the second hydride transfer in CPR occurs at essentially the same rate as that seen for hydride transfer in the isolated FAD-domain.

As described above for the isolated FAD-domain, the observed rates for the first hydride transfer from NADPH to CPR *increase* on lowering the NADPH concentration below 100 μM (Figure 10). In the pseudo-first-order regime, the observed rate of transfer of the second hydride anion is independent of NADPH concentration (Figure 10). It has not been possible to investigate the observed rate for the second hydride transfer at low NADPH concentrations, due to progressive loss of the kinetic phases at 600 and 450 nm that report on this reaction (e.g., see Figure 8, panel B). One might expect, however, that a similar concentration-dependence holds for the transfer of the second hydride ion to CPR as for the first.

Steady-state assays of cytochrome *c* reduction by human CPR reveal a simple hyperbolic relationship on NADPH concentration, with an apparent Michaelis constant of 3.6 ± 0.5 μM and turnover number of 12 ± 0.4 s^{-1} (at 50 μM cytochrome *c*). The rate of turnover is significantly faster than the rate of the second hydride transfer in the pseudo-first-order regime observed in stopped-flow studies (3 s^{-1}; Figure 10). The data suggest that the reduction level of CPR does not extend to the four-electron level in steady-state reactions, since the expected turnover number would be ~3 s^{-1}. Moreover, steady-state assays reveal that activity is not inhibited at higher NADPH concentrations, suggesting that CPR is not reduced to the four-electron level even at high concentrations (160 μM) of NADPH. Our steady-state data is consistent with the FMN semiquinone acting as electron donor to cytochrome *c*, as also demonstrated for house fly CPR (*43*).

The kinetic mechanism of full-length CPR can be summarized as shown in Scheme 2. In contrast to the FAD-domain, we found no evidence for discrete charge-transfer intermediates in full-length CPR. However, the dependence of hydride transfer in full-length CPR on NADPH concentration is similar to that seen with the isolated FAD-domain and indicates that intermediates prior to hydride transfer (plausibly charge-transfer intermediates) may also accumulate in CPR (see Discussion). In Scheme 2, the approximate equilibrium distributions of the two-electron-reduced form following the first hydride transfer are shown. Over very long time excursions (100 s), further spectral changes occur in CPR during stopped-flow studies (Figure 11). These absorption changes display complex kinetics and, as discussed for the rabbit enzyme (*34*), most likely represent thermodynamic relaxation of the system via a series of equilibration reactions; these latter reactions are of no catalytic relevance and they are therefore not included in Scheme 2.

DISCUSSION

The mechanism of electron flow from NADPH to cytochrome P450, mediated by CPR, has been the focus of detailed studies for a number of years. Early studies concentrated on the rabbit hepatic enzyme. The air-stable semiquinone form of CPR was shown to be a one-electron-reduced enzyme species (*8*), and the reduction potentials of the individual flavin couples have been reported (*32*). These potentials have been assigned to the relevant flavin centers following selective removal of FMN from detergent-solubilized enzyme (*9*, *44*). Stopped-flow studies with rabbit hepatic CPR demonstrated that reduction with NADPH occurs in three phases (*34*): a fast first phase yielding an equilibrium mixture of about 70% ($FMNH_2$, FAD) and 30% disemiquinone (FMNH•, FADH•); a second phase yielding about 65% ($FMNH_2$, $FADH_2$), 24% ($FMNH_2$, FAD), and 11% (FMNH•, FADH•); and a third slow phase representing thermodynamic equilibration of the species formed in the second phase.

In this and the preceding paper in this issue (*1*), the first detailed studies of the kinetics and thermodynamics of electron flow in human CPR are described. Our studies have taken advantage of the availability of the isolated FMN- and FAD-domains of human CPR (*24*), which has enabled the first detailed examination of the redox properties of these individual domains. The potentials of the two flavin centers in human CPR are in broad agreement with those determined for the rabbit enzyme (*1*). Our kinetic studies with full-length human CPR also find parallels with those reported with the rabbit enzyme, to the extent that three kinetic phases are found to accompany the reaction of CPR with NADPH in stopped-flow experiments. We have demonstrated the reversibility of the individual steps in the reductive half-reaction of human CPR, as demonstrated in house fly CPR (*45*) and in the work of Oprian and Coon on rabbit CPR

Scheme 2

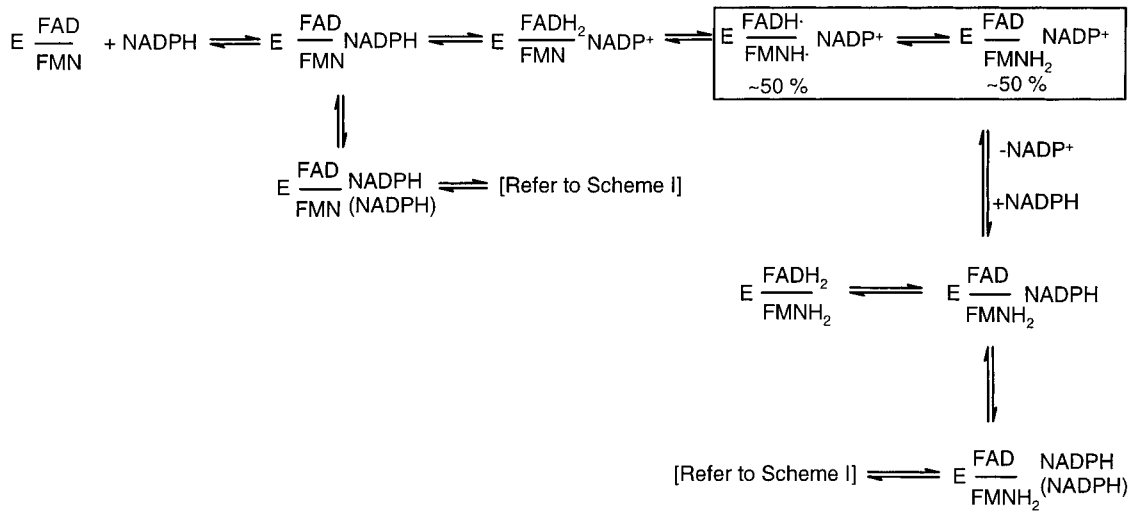

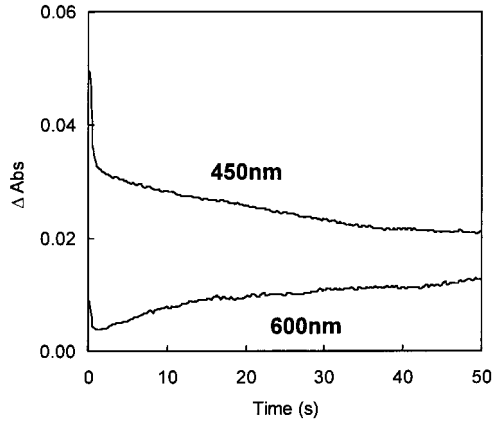

FIGURE 11: Spectral changes occurring in CPR following prolonged incubation of the enzyme with NADPH. Conditions as in Figure 8. Appearance of the blue semiquinone (600 nm) and loss of signature at 450 nm likely represents comproportionation of species to reach the thermodynamically stable state.

(*34*). On the basis of the midpoint potentials of human CPR and its constituent domains (*1*), the distribution of enzyme species at the end of each kinetic phase will be broadly similar to those reported for the rabbit enzyme.

Our detailed kinetic studies have also revealed new features of the reductive half-reaction of CPR. In particular, we have demonstrated that human CPR (and the isolated FAD-domain) is inhibited at high NADPH concentration, enabling us to construct new kinetic schemes (Schemes 1 and 2) that accommodate a complex containing two NADPH molecules as a branch from the main reaction pathway. The structural basis for this inhibition by NADPH remains to be established. However, our stopped-flow fluorescence studies with CPR indicate rapid changes in tryptophan fluorescence prior to hydride transfer that likely report on the movement of Trp-676, which is located near the isoalloxazine ring of the FAD, during the binding of NADPH. We suggest the binding of a second NADPH molecule may interfere with the dynamics of this side chain movement, thus impeding hydride transfer. The role of this tryptophan residue in flavin reduction is currently being investigated through the study of appropriate mutant CPR enzymes.

The midpoint potential of the isolated FAD-domain is essentially isopotential with the same domain contained in full-length CPR (*1*), and the kinetics of reduction of the domain are similar to those of the second hydride transfer reaction in full-length CPR. These observations demonstrate that functionally the isolated FAD-domain is an excellent model of the FAD-domain contained in CPR, thus establishing the validity of studying the isolated FAD-domain to gain additional insight into the functioning of CPR. We have demonstrated that binding of NADPH to the FAD-domain occurs via the formation of two discrete NADPH−FAD-domain charge-transfer complexes (CT1 and CT2). The first (CT1) is formed rapidly and is almost completely formed in the dead-time (1.2 ms) of the stopped-flow apparatus. The second charge-transfer species (CT2) also forms quickly (about 200 s^{-1}) and leads to a further enhancement in charge-transfer signature in the long-wavelength region of the spectrum. We suggest that similar charge-transfer species also accumulate in full-length CPR but that their formation is masked by the relatively large spectral changes accompanying the formation of the di-semiquinonoid form of CPR, the spectral signature of which overlaps with that expected for charge-transfer species in the long-wavelength region. The stopped-flow fluorescence studies of the isolated FAD-domain have also aided the deconvolution of the more complex fluorescence changes occurring in full-length CPR immediately after the mixing event. In the isolated FAD-domain, we observe a single rapid phase prior to hydride transfer that we attribute to a change in environment of Trp-676 on the binding of NADPH. In full-length CPR several phases are seen in our stopped-flow studies, which can be assigned (with some confidence) to the NADPH-binding and hydride transfer reactions, by comparison with the fluorescence changes occurring in the isolated FAD-domain and absorption changes in full-length CPR.

We have demonstrated the reversibility of the hydride transfer reaction in the isolated FAD-domain by performing stopped-flow experiments with two-electron-reduced FAD-domain and $NADP^+$. The reversibility of this reaction would be anticipated on the basis of the relative redox potentials of NADPH and FAD but is interesting from an evolutionary standpoint. As noted above, the FAD-domain shows a clear structural similarity to the flavoenzyme ferredoxin-$NADP^+$ reductase (FNR). The physiological role of the majority of the enzymes of this family is to catalyze the reduction of

$NADP^+$. Only enzymes that contain a flavodoxin-like FMN-domain in addition to an FNR-like FAD-domain, such as CPR, *Bacillus megaterium* cytochrome P450 BM-3 (*46*), bacterial NADPH-sulfite reductase (*47*), and nitric oxide synthase (*48*) operate in the direction of NADPH oxidation. As discussed in the preceding paper in this issue (*1*), the observed rapid transfer of an electron from FAD to FMN is likely to be a key factor in this "reversal of direction" within this family of FAD-containing enzymes.

In FNR, a tyrosine residue (Tyr-308 in pea FNR) shields the isoalloxazine ring of FAD from the nicotinamide cofactor, in an analogous fashion to Trp-677 in rat CPR (*27*), and the binding of $NADP^+$ involves an energetically unfavorable displacement of the tyrosine side chain to allow access of the nicotinamide to the FAD (*49*). Structures of complexes of $NADP^+$ and NADPH with FNR mutants reveal that the nicotinamide ring is not parallel to the flavin isoalloxazine ring, as it is in glutathione reductase (*50*, *51*), NADH peroxidase (*52*), and quinone reductase (*53*) but lies against the isoalloxazine ring at an angle of about 30°, with the C4 atom 3 Å from the flavin N5. Given the structural similarity of the FAD-domain of CPR with FNR, CPR may provide a second example of a flavoenzyme in which the nicotinamide cofactor does not form the more common parallel interaction with the flavin isoalloxazine ring.

ACKNOWLEDGMENT

We are grateful to Samantha Jones and Daniel H. Craig for technical assistance.

REFERENCES

1. Munro, A., Noble, M., Robledo, L., Daff, S., and Chapman, S. (2001) *Biochemistry 40*, 1956−1963.
2. Ortiz de Montellano, P. (1995) Plenum Press, New York.
3. Philips, A., and Langdon, R. (1962) *J. Biol. Chem. 237*, 2652−2660.
4. Lu, A., Junk, K., and Coon, M. (1969) *J. Biol. Chem. 244*, 3714−3721.
5. Porter, T. D. (1991) *Trends Biochem. Sci. 16*, 154−158.
6. Shen, A., and Kasper, C. B. (1993) In *Handbook of Experimental Pharmacology* (Schenkman, J. B., and Grein, H., Eds.) pp 35−59, Springer-Verlag, New York.
7. Strobel, H., Hodgson, A., and Shen, S. (1995) In *Cytochrome P450: Structure, Mechanism and Biochemistry* (Ortiz de Montellano, P., Ed.) pp 225−244, Plenum Press, New York.
8. Iyanagi, T., and Mason, H. S. (1973) *Biochemistry 12*, 2297−2307.
9. Vermilion, J. L., Ballou, D. P., Massey, V., and Coon, M. J. (1981) *J. Biol. Chem. 256*, 266−277.
10. Enoch, H. G., and Strittmatter, P. (1979) *J. Biol. Chem. 254*, 8976−81.
11. Schacter, B. A., Nelson, E. B., Marver, H. S., and Masters, B. S. (1972) *J. Biol. Chem. 247*, 3601−7.
12. Ilan, Z., Ilan, R., and Cinti, D. L. (1981) *J. Biol. Chem. 256*, 10066−72.
13. Masters, B. S. S. (1980) in *Enzymatic Basis of Detoxification* (Jakoby, W., Ed.) pp 183−200, Academic Press, Inc., Orlando, FL.
14. Kurzban, G. P., and Strobel, H. W. (1986) *J. Biol. Chem. 261*, 7824−7830.
15. Keyes, S. R., Fracasso, P. M., Heimbrook, D. C., Rockwell, S., Sligar, S. G., and Sartorelli, A. C. (1984) *Cancer Res. 44*, 5638−43.
16. Bligh, H. F., Bartoszek, A., Robson, C. N., Hickson, I. D., Kasper, C. B., Beggs, J. D., and Wolf, C. R. (1990) *Cancer Res. 50*, 7789−92.
17. Bartoszek, A., and Wolf, C. R. (1992) *Biochem. Pharmacol. 43*, 1449−57.
18. Walton, M. I., Wolf, C. R., and Workman, P. (1992) *Biochem. Pharmacol. 44*, 251−9.
19. Patterson, A. V., Barham, H. M., Chinje, E. C., Adams, G. E., Harris, A. L., and Stratford, I. J. (1995) *Br. J. Cancer 72*, 1144−50.
20. Griffith, O. W., and Stuehr, D. J. (1995) *Ann. Rev. Physiol. 57*, 707−736.
21. Leclerc, D., Wilson, A., Dumas, R., Gafuik, C., Song, D., Watkins, D., Heng, H. H., Rommens, J. M., Scherer, S. W., Rosenblatt, D. S., and Gravel, R. A. (1998) *Proc. Natl. Acad. Sci. U.S.A. 95*, 3059−64.
22. Paine, M. J., Garner, A. P., Powell, D., Sibbald, J., Sales, M., Pratt, N., Smith, T., Tew, D. G., and Wolf, C. R. (2000) *J. Biol. Chem. 275*, 1471−8.
23. Porter, T. D., and Kasper, C. B. (1986) *Biochemistry 25*, 1682−1687.
24. Smith, G. C. M., Tew, D. G., and Wolf, C. R. (1994) *Proc. Natl. Acad. Sci. U.S.A. 91*, 8710−8714.
25. Narayanasami, R., Horowitz, P. M., and Masters, B. S. (1995) *Arch. Biochem. Biophys. 316*, 267−74.
26. Hodgson, A. V., and Strobel, H. W. (1996) *Arch. Biochem. Biophys. 325*, 99−106.
27. Wang, M., Roberts, D. L., Paschke, R., Shea, T. M., Masters, B. S., and Kim, J. J. (1997) *Proc. Natl. Acad. Sci. U.S.A. 94*, 8411−8416.
28. Zhao, Q., Modi, S., Smith, G., Paine, M., McDonagh, P. D., Wolf, C. R., Tew, D., Lian, L. Y., Roberts, G. C. K., and Driessen, H. P. (1999) *Protein Sci. 8*, 298−306.
29. Barsukov, I., Modi, S., Lian, L.-Y., Sze, K. H., Paine, M. J. I., Primrose, W. U., Wolf, C. R., and Roberts, G. C. K. (1997) *J. Biomol. NMR 10*, 63−75.
30. Watenpaugh, D. K., Sieker, L. C., and Jensen, L. H. (1973) *Proc. Natl. Acad. Sci. U.S.A. 70*, 3857−3860.
31. Karplus, P. A., Daniels, M. J., and Herriott, J. R. (1991) *Science 251*, 60−66.
32. Iyanagi, T., Makino, N., and Mason, H. S. (1974) *Biochemistry 13*, 1701−1710.
33. Iyanagi, T., Makino, R., and Anan, F. K. (1981) *Biochemistry 20*, 1722−1730.
34. Oprian, D. D., and Coon, M. J. (1982) *J. Biol. Chem. 257*, 8935−8944.
35. Guengerich, F. P., and Johnson, W. W. (1997) *Biochemistry 36*, 14741−14750.
36. Bhattacharyya, A. K., Lipka, J. J., Waskell, L., and Tollin, G. (1991) *Biochemistry 30*, 759−765.
37. Zhao, Q., Smith, G., Paine, M., Wolf, C. R., Modi, S., Lian, L.-Y., Primrose, W. U., Roberts, G. C. K., and Driessen, H. (1996) *J. Struct. Biol. 116*, 320−325.
38. Modi, S., Gilham, D. E., Sutcliffe, M. J., Lian, L.-Y., Primrose, W. U., Wolf, C. R., and Roberts, G. C. K. (1997) *Biochemistry 36*, 4461−4470.
39. Klatt, P., Schmidt, K., Werner, E. R., and Mayer, B. (1996) *Methods Enzymol. 268*, 358−365.
40. Macheroux, P. (1999) In *Flavoprotein Protocols* (Chapman, S., and Reid, G., Eds.) pp 1−7, Humana Press.
41. Craig, D. H., Moody, P. C. E., Bruce, N. C., and Scrutton, N. S. (1998) *Biochemistry 37*, 7598−7507.
42. Batie, C. J., and Kamin, H. (1986) *J. Biol. Chem. 261*, 11214−11223.
43. Murataliev, M. B., and Feyereisen, R. (1999) *FEBS Lett. 453*, 201−4.
44. Vermilion, J. L., and Coon, M. J. (1978) *J. Biol. Chem. 253*, 8812−8819.
45. Murataliev, M. B., and Feyereisen, R. (2000) *Biochemistry 39*, 5066−74.
46. Ruettinger, R., Wen, L., and Fulco, A. (1989) *J. Biol. Chem. 264*, 10987−10995.
47. Ostrowski, J., Barber, M., Rueger, D., Miller, B., Siegel, L., and Kredich, N. (1989) *J. Biol. Chem. 264*, 15796−15808.

48. Geller, D., Lowenstein, C., Shapiro, R., Nussler, A., Di Silvio, M., Wang, S., Nakayama, D., Simmons, R., Snyder, S., and Billiar, T. (1989) *Proc. Natl. Acad. Sci. U.S.A. 90*, 3491−3495.
49. Deng, Z., Aliverti, A., Zanetti, G., Arakaki, A. K., Ottado, J., Orellano, E. G., Calcaterra, N. B., Ceccarelli, E. A., Carrillo, N., and Karplus, P. A. (1999) *Nat. Struct. Biol. 6*, 847−853.
50. Karplus, P. A., and Schulz, G. E. (1989) *J. Mol. Biol. 210*, 163−180.
51. Mittl, P. R. E., Berry, A., Scrutton, N. S., Perham, R. N., and Schulz, G. E. (1994) *Protein Sci. 3*, 1504−1514.
52. Stehle, T., Claiborne, A., and Schulz, G. E. (1993) *Eur. J. Biochem. 211*, 221−226.
53. Li, R., Bianchet, M. A., Talalay, P., and Amzel, L. M. (1995) *Proc. Natl. Acad. Sci. U.S.A. 92*, 8846−8850.

BI001719M